ISSN 1062-8738, Bulletin of the Russian Academy of Sciences: Physics, 2022, Vol. 86, No. 3, pp. 266–274. © Allerton Press, Inc., 2022.
Russian Text © The Author(s), 2022, published in Izvestiya Rossiiskoi Akademii Nauk, Seriya Fizicheskaya, 2022, Vol. 86, No. 3, pp. 340–348.

Magnetic Substorms and Auroras at the Polar Latitudes of Spitsbergen: Events of December 17, 2012

I. V. Despirak[a], *, N. G. Kleimenova[b], A. A. Lubchich[a], L. M. Malysheva[b], L. I. Gromova[c], A. V. Roldugin[a], and B. V. Kozelov[a]

[a] *Polar Geophysical Institute, Apatity, 184209 Russia*
[b] *Schmidt Institute of Physics of the Earth, Moscow, 123995 Russia*
[c] *Pushkov Institute of Terrestrial Magnetism, Ionosphere, and Radio Wave Propagation, Moscow, 108840 Russia*
**e-mail: despirak@gmail.com*

Received October 15, 2021; revised November 5, 2021; accepted November 22, 2021

Abstract—A comparative analysis is performed of the development of two polar substorms observed over Spitsbergen on December 17, 2012. Magnetometer data from the SuperMAG and IMAGE networks is used in combination with data from the AMPERE satellites and observations of the aurora made by the Barentsburg observatory (Spitsbergen archipelago). It is shown that the superpositioning of the evening polar substorm and the poleward leap of the western edge of the electrojet of the nighttime auroral substorm differed from a typical night polar substorm in the forms of the auroras, the distribution of field-aligned currents, and their midlatitude effects.

DOI: 10.3103/S1062873822030091

INTRODUCTION

It is known that substorms can be observed at both auroral and very high geomagnetic latitudes (>70° MLAT) [1–4]. According to the dynamics of the auroral oval, this can happen (1) during disturbed periods when the auroral oval expands strongly and disturbances are recorded from low to high latitudes, and (2) under quiet conditions where the auroral oval is contracted and moves to high latitudes [5]. In the first case, expanded ("high-latitude") substorms are observed on the extended oval [6–9]. In the second, there are so-called substorms on the contracted oval [10, 11]. The morphological characteristics of such substorms, and their relationship to Pi2 geomagnetic pulsations and auroras, were studied in detail in [12], where the term "polar" substorms was proposed for them.

The dependence of such substorms on solar activity, magnetic storms, and the large-scale structure of the solar wind was studied in [13–15]. It was shown that polar substorms are observed at low velocities of the solar wind after the passing of a recurrent high-velocity flow, during a slow flow of the solar wind under calm conditions, or in the late recovery phase of a geomagnetic storm. It was shown in [16] that a polar substorm has features not typical of a classical substorm. These include starting at the polar boundary of the oval between the downward and upward field-aligned current, and auroras developing in the form of torches and large-scale spiral structures. It may therefore be said that the study of polar substorms has just begun and requires further research.

The aim of this paper was to analyze the substorm disturbances of December 17, 2012 (the evening disturbance at ~16:00–17:00 UT and the near-midnight disturbance at ~21:30 UT), observed on the Spitsbergen archipelago (geomagnetic midnight at ~21:00 UT) and their accompanying auroras.

EXPERIMENTAL DATA

This study is based on an analysis of ground-based observation data using the global network of SuperMAG magnetometers (http://supermag.jhuapl.edu/) [17]; the meridional Scandinavian IMAGE station network (http://space.fmi.fi/image/) [18]; satellite data from the AMPERE project (Active Magnetosphere and Planetary Electrodynamics Response Experiment, http://www.ampere.jhuapl.edu); and data from detectors of the Polar Geophysical Institute installed at the Barentsburg observatory on the Spitsbergen archipelago (BAB, 75.6° MLAT). The development of the magnetic substorm was monitored using instantaneous map of the global spatial distribution of the westward electrojet, constructed with data from the SuperMAG network, and maps of the distribution of magnetic disturbances in the ionosphere (at an altitude of 680 km), obtained using data from the *Iridium* communication satellites of the AMPERE project and field-aligned currents calculated from these observations. The AMPERE project includes

simultaneous recording of the magnetic field by 66 satellites at 12 meridional profiles [19, 20]. The maps are constructed every 2 min with averaging over 10 min. To study the auroral dynamics, we used keograms in north–south direction and selected full-frame images from the all-sky camera (http://aurora.pgia.ru:8071/). Pi1B geomagnetic pulsations [21, 22] were observed using an induction magnetometer installed at the Barentsburg observatory. The data used were spectrograms in the frequency band of 0.01 to 3 Hz. The conditions in the solar wind and the interplanetary magnetic field (IMF) were determined using OMNI 1-min CDAWeb data (http://cdaweb.gsfc.nasa.gov/).

For our analysis, we selected two cases of substorm disturbances observed simultaneously over the Spitsbergen archipelago on December 17, 2012, by the magnetometers and all-sky cameras. Figure 1a presents the interplanetary conditions from 05:00 to 24:00 UT on December 17, 2012. Figure 1b shows variations of the magnetic field from 14:00 to 24:00 UT for the stations of the IMAGE network (top) and the Dixon (DIK, 69.3° MLAT) and Tixi (TIK, 66.7° MLAT) stations (bottom). The black triangle marks midnight. The IMAGE stations were in the evening sector; the DIK and TIK stations, in the midnight sector. The considered events are marked by vertical red lines (Fig. 1a) or ovals (Fig. 1b). Before they occured, two bow shock waves (forward and reverse) were observed, that caused jumps in the solar wind parameters. A weak high-velocity flow ($V \sim 500$ km/s) and an enchancement in dynamic pressure from ~2 to ~5 nPa was recorded ~5–6 h prior to the onset of the first disturbance. This likely led to the development of three strong aural substorms from 09:00 to ~17:00 UT (SML ~ −1300, −1000, and −700 nT).

We can see that both events were recorded under quiet conditions ($SYM/H > -20$ nT) at positive B_Z and B_Y of the IMF and a low solar wind velocity (~450 km/s). The first event started at increased values of the IMF ($B_T \sim 8$ nT), a solar wind velocity of ~460 km/s, and after the IMF B_Z-component had changed from negative to positive values. The second polar substorm occurred under quieter conditions. The magnitude of the magnetic field fell to ~6 nT, the solar wind was slower (~400 km/s), the IMF B_Z-component was positive, and there was no jump in dynamic pressure. Note that the first event was observed at Kp = 2, when the auroral oval was relatively disturbed. The second substorm was observed under very quiet conditions (Kp = 0) where the auroral oval contracted poleward.

The IMAGE magnetograms show that at the Bear Island station (BJN, ~71.9° MLAT), the disturbances started around 16:10 UT and quickly developed poleward to the Ny-Ålesund station (NAL, ~76.6° MLAT); there were no negative bays at lower latitudes. This disturbance was likely poleward expansion (a so-called poleward leap [23]) of the western edge of the electrojet of the auroral substorm observed in Tixi (TIK) and then in Dixon (DIK). Figure 1b shows this substorm began at the TIK station at ~15:00 UT. Three intensifications (~15:50, ~16:12; ~16:30 UT) were recorded at the DIK station. There was a short impulse of ~−730 nT at ~16:12 UT that, probably, contributed to the amplitude of the substorm at TIK and the development of the poleward leap, along with variations in the SML index (Fig. 1a).

No disturbances were observed at the DIK and TIK stations during the second substorm at ~21:30 UT. This was a classical polar substorm for which disturbances of ~−200 nT were recorded only at high latitudes (from BJN to NAL).

OBSERVATIONS IN BARENTSBURG

Figure 2 presents data from the all-sky camera and induction magnetometer installed at the Barentsburg observatory (BAB) for the intervals of 15:30–18:00 UT (left) and 20:00–22:00 UT (right): (a) variations of X- and Z- components of the magnetic field; (b) spectrograms in the frequency band of 0.01 to 3 Hz; (c) keograms, and (d) selected images from the all-sky camera.

During the first event, the disturbance started at ~16:10 UT. The amplitude of the magnetic bay rose sharply (to ~−220 nT) at ~16:48 UT, with its maximum being recorded at ~16:53 UT. The Z-component changed its sign at that moment (from positive to negative values), indicating the westward electrojet was located over Barentsburg. Pi1B geomagnetic pulsations (0.08–3 Hz) began at ~16:10 UT and consisted of several peaks (~16:25, ~16:35, ~16:50 UT). The maximum intensity of pulsations was observed during the third peak. The pulsation peaks correspond to three minima in the variations of the X-component of the geomagnetic field at the BJN-NAL stations (Figs. 1b and 3a) and three intensifications in auroras (Figs. 2c, 2d). The auroras appeared at the southern limit of the all-sky camera view at ~16:17 UT. They then intensified, extended in azimuth, and moved slightly poleward at ~16:24–16:27 UT, but this took place far from the zenith. This period corresponds to the time of the first peak of Pi1B pulsations. There was a new intensification of auroras at the southern limit of the image at ~16:30 UT. The development took the form of a spiral that reached its maximum at ~16:35 UT, which corresponds to the second peak of Pi1B pulsations. The auroras intensified again at ~16:41 UT, modifying their shape and moving gradually poleward. After ~16:45 UT, they quickly spread poleward and passed through the zenith of the station.

The second substorm began in the near-midnight sector from a small disturbance (~−40 nT) at ~20:50 UT. A magnetic bay with an intensity of ~−140 nT was recorded at ~21:20 UT, and a small intensification was observed at ~21:35 UT. At this time, the Z-component displayed positive bays, indicating that the westward electrojet was located to the south of BAB. Pi1B pul-

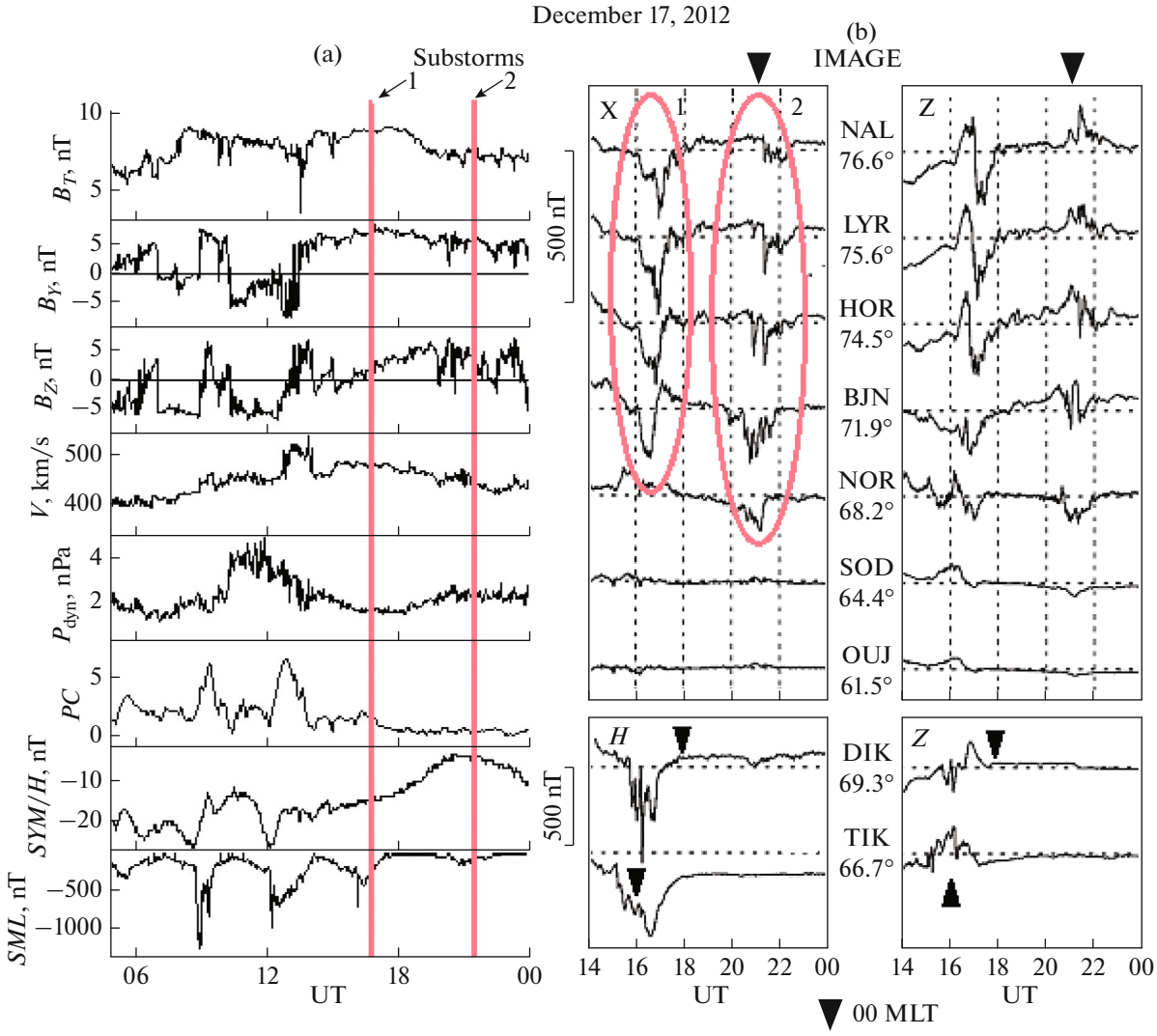

Fig. 1. Interplanetary parameters and variations in the Earth's magnetic field on December 17, 2012 (the solar wind and IMF parameters, and the geomagnetic indices from 05:00 to 24:00 UT). (a) Top to bottom: magnitude B_T of the magnetic field, IMF B_Y and B_Z components, velocity and dynamic pressure of solar wind, *PC*, *SYM/H* and *SML* geomagnetic indices; variations in the *X*- and *Z*-components of the magnetic field of ground-based magnetic stations from the IMAGE network (upper panel) and the *H*- and *Z*-components at the Dixon and Tixi stations (bottom panel) from 14:00 to 24:00 UT on December 17, 2012. (b) Moments of observing the polar substorms are indicated by vertical red lines (left) and ovals (right).

sations began at ~20:40 UT, with several peaks occurring (at ~20:55, ~21:20, and ~21:35 UT) as in the first case. This conforms to three intensifications in the variations of the *X*-component of the geomagnetic field in BAB (Fig. 2a) and at the BJN-NAL stations (Figs. 1b and 4a), and to the intensifications in auroras (Fig. 2d). Unfortunately, it was cloudy in Barentsburg at this time, so it was difficult to monitor the auroral dynamics accurately. Auroras appeared at the southern limit of the all-sky camera view at ~20:40 UT. They then extended in azimuth and moved poleward until ~21:01:30 UT. This occurred in the southern part of the image, confirming that at this time the substorm developed southward of BAB. New poleward movement of the arcs began ~21:18:20 UT and lasted until ~21:23 UT, when the auroras almost reached the image's zenith. The arcs also intensified at ~21:27 UT and then jumped poleward (break-up), with the arcs passing through the station's zenith farther northward. At this time, however, the clouds interfered with observations. We could only see the arcs had already passed through the zenith of the station at ~21:33:10 UT. They then continued moving northward, and a spiral structure formed north of the zenith at ~21:41 UT.

MAGNETIC DISTURBANCES DURING THE FIRST AND SECOND EVENT

Figures 3 and 4 show the development of magnetic disturbances, according to data from the AMPERE

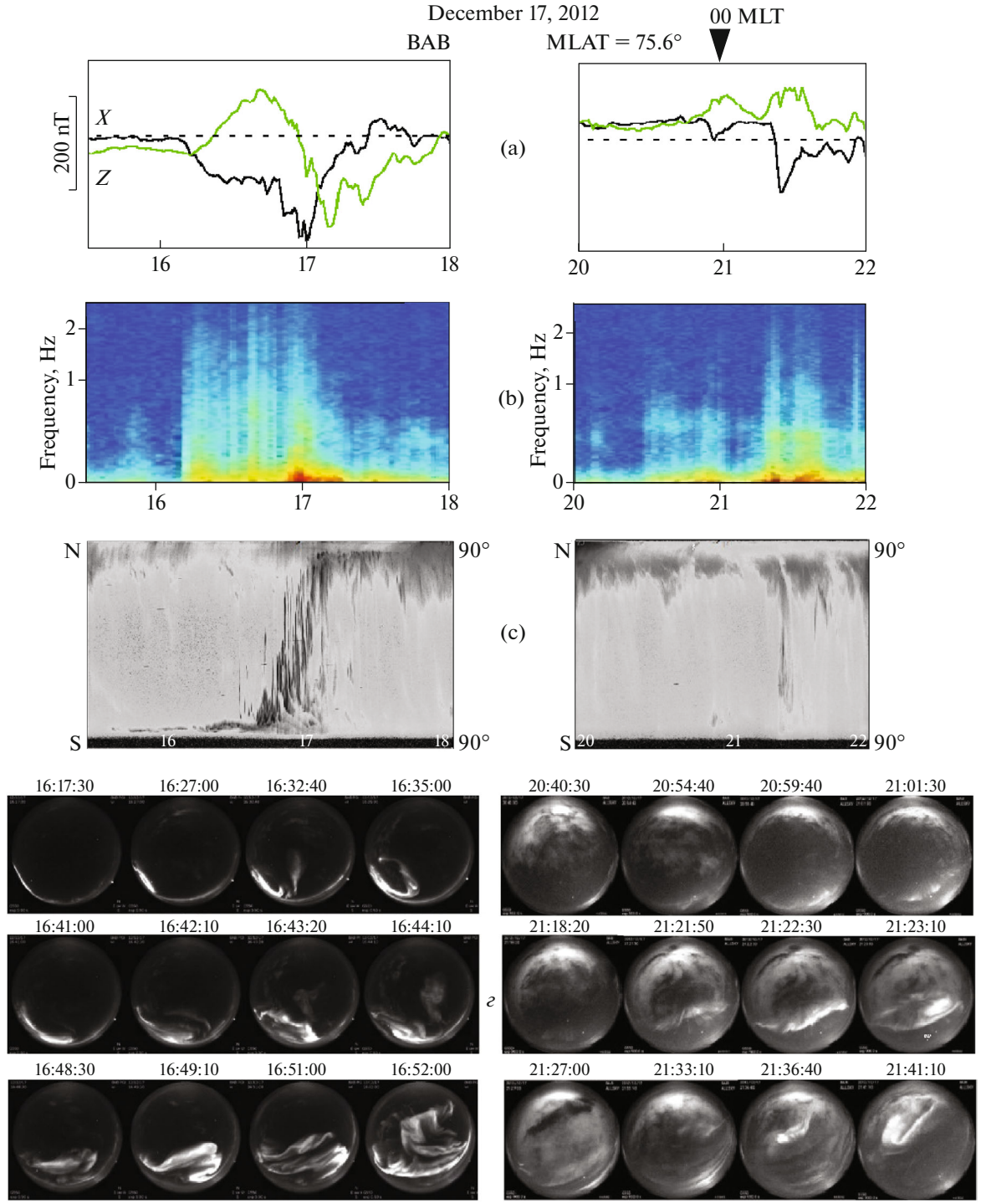

Fig. 2. Data from the Barentsburg observatory for December 17, 2012, during the first substorm from 15:30 to 18:00 UT (left) and the second substorm from 20:00 to 22:00 UT (right). (a) Variations in the *X*- and *Z*-components of the magnetic field; (b) spectrograms in the frequency band of 0.01 to 3 Hz; (c) keograms obtained from all-sky camera data; and (d) selected all-sky camera images from 16:17:30 to 16:52:00 UT and 20:40:30 to 21:41:10 UT.

satellites and the IMAGE and SuperMAG networks. Figure 3a shows variations of the *X*-component of the magnetic field from 15:00 to 19:00 UT on December 17, 2012, at the IMAGE stations (NOR–NAL, from ~68.2° to ~76.6° MLAT). We see that a negative bay (~−80 nT) began at stations BJN–NAL at ~16:10 UT. Its onset coincided with a large negative impulse at the DIK station (Fig. 1b) and a sharp intensification of the

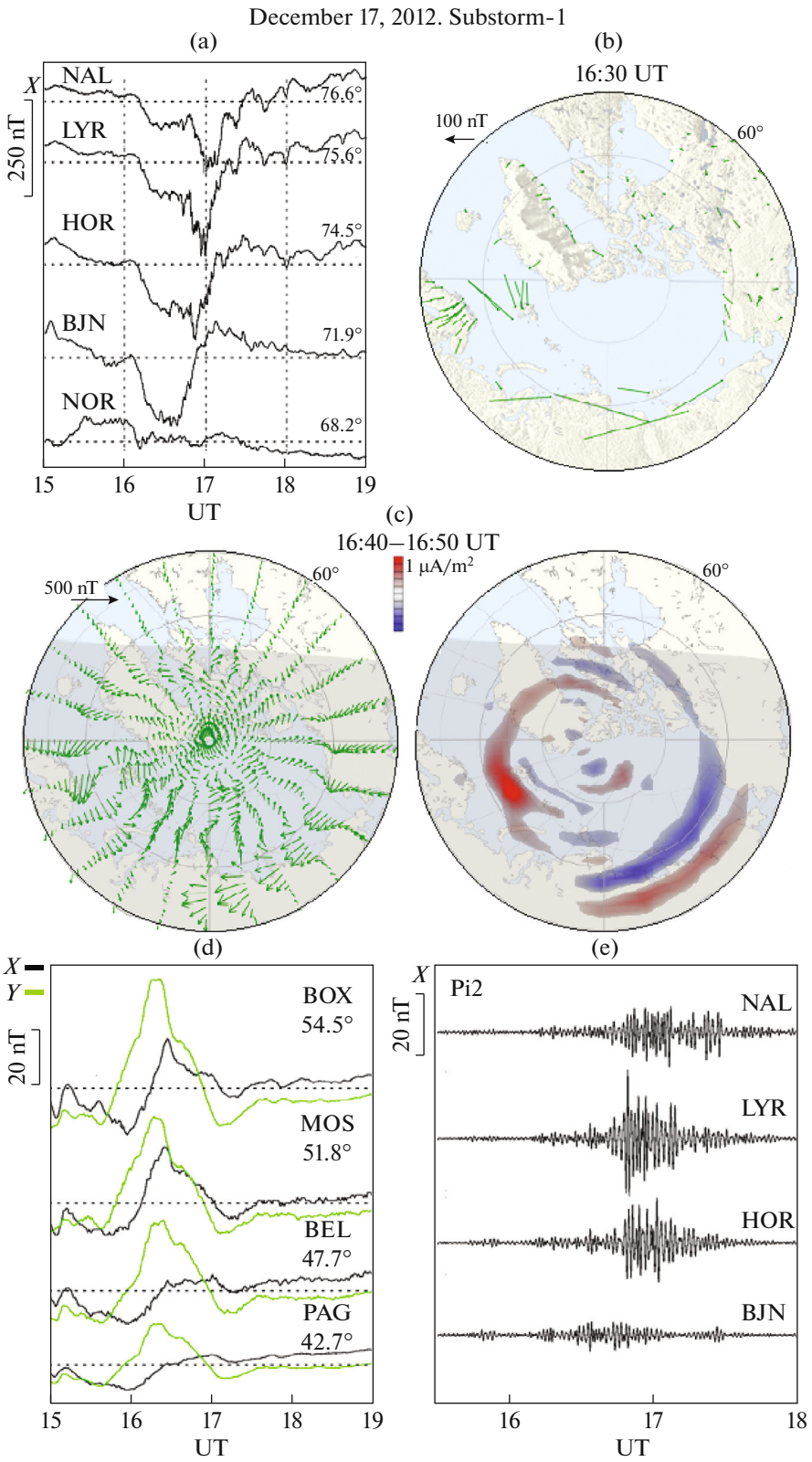

Fig. 3. Variations in the *X*- and *Z*-components of the geomagnetic field at several ground-based magnetic stations, plus global maps of magnetic disturbances for the period of the first complex disturbance (15:00–19:00 UT on December 17, 2012) (a) from the IMAGE network and (d) the SuperMAG network; (b) instantaneous map of magnetic vectors at 16:30 UT, constructed from SuperMAG data; (c) maps of the distribution of magnetic disturbances and field-aligned currents at the altitude of AMPERE satellites for 16:40–16:50 UT; (e) Pi2 geomagnetic pulsations for high-latitude IMAGE stations. The geomagnetic coordinates (MLAT) of the stations are given next to their names. Midnight is at the bottom of the maps; noon is at the top. The downward current is shown in blue; the upward current is marked in red.

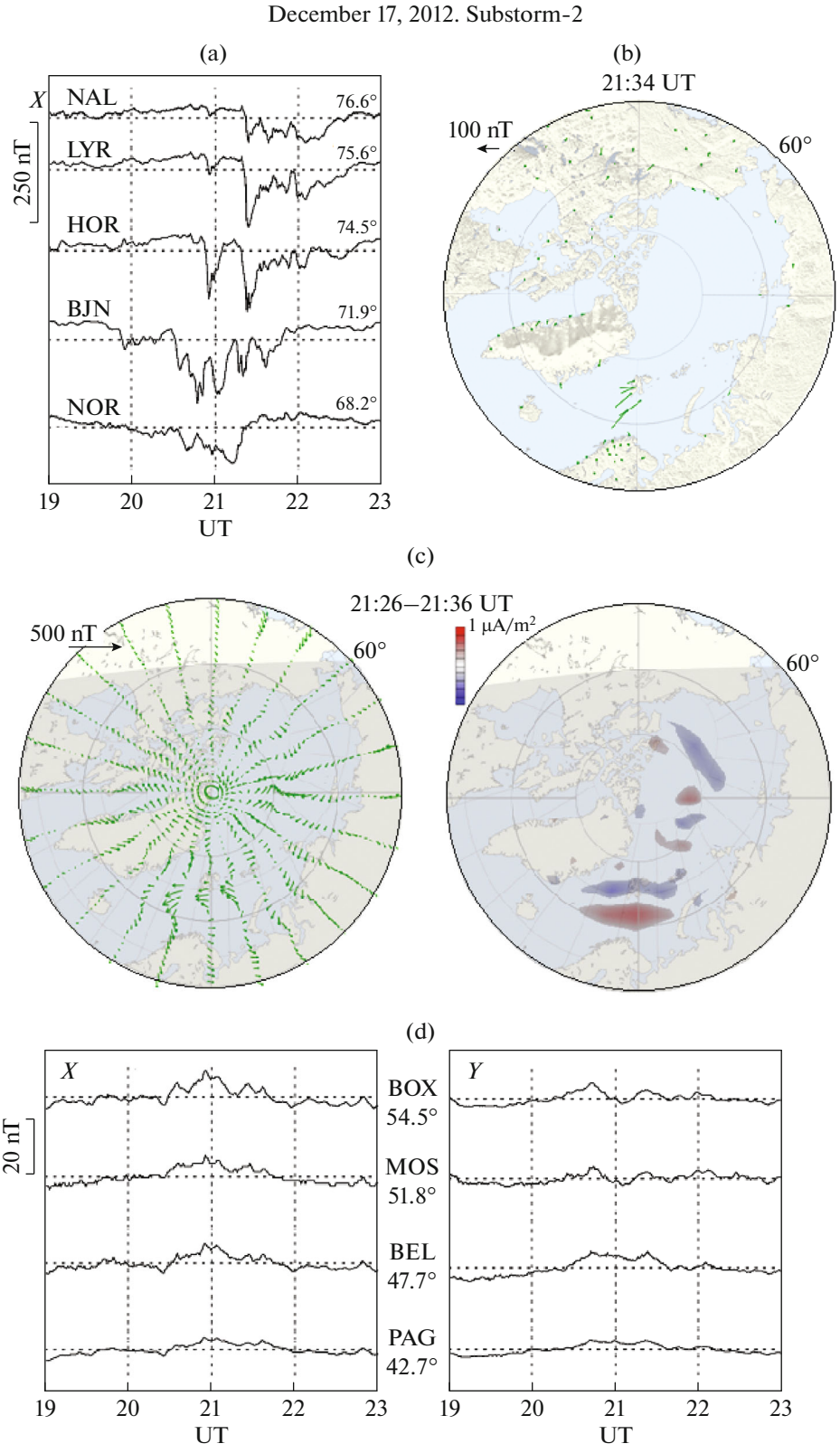

Fig. 4. Variations in the *X*- and *Z*-components of the geomagnetic field at several ground-based magnetic stations and global maps of magnetic disturbances for the period 19:00 to 23:00 UT of the second substorm of December 17, 2012.

substorm in the near-midnight sector (the TIK station). There was also the northward turn of the IMF B_Z at this time. This would normally result in contraction of the auroral oval, so the high-latitude magnetic disturbances at the IMAGE meridian can be considered the westward expansion of the electrojet of the night substorm and the development of the so-called poleward leap [23] at the western edge of the electrojet. The maximum amplitudes were observed at ~16:30 UT at BJN.

Figure 3a shows that at the HOR–NAL stations (i.e., poleward of BJN), the amplitude of the bay jumped to ~–220 nT) at ~16:40 UT, indicating the start of a new disturbance that could be related morphologically to a polar substorm [12]. This disturbance was observed at IMF $B_Z > 0$ and only at latitudes above 72° MLAT (HOR–NAL). At lower latitudes, the bay was not observed at all. Figure 3e shows that the onset of the bay and its subsequent development were accompanied by a burst of intense Pi2 geomagnetic pulsations. This is atypical for a poleward leap [23], but it is typical for a polar substorm [12]. The start of the disturbance was followed not only by rapid growth of the bay, but by rapid increases in the amplitudes of Pi1B (Fig. 2b) and Pi2 (Fig. 3e) geomagnetic pulsations as well, along with brightening (Fig. 2d) and rapid poleward movement of the auroras (Fig. 2c). This is typical of a polar substorm [12]. Data from the system of AMPERE satellites testifies to the emergence of intense upward field-aligned currents in this region (Fig. 3c).

The new magnetic disturbance that began at ~16:40 UT can thus be considered a polar substorm caused by intensification of field-aligned currents in the poleward leap region at the western edge of the night substorm electrojet.

In the first event, positive magnetic bays were recorded in the *X*-component at subauroral (~10–15 nT; these data are not provided here) and middle latitudes (~20–25 nT, Fig. 3d). Note that the positive bays were more intense in the *Y*-component of the field: ~40 nT at the Borok (BOX, 54.5° MLAT) and Moscow (MOS, 51.8° MLAT) stations, and ~30 nT at the Belsk (BEL, 47.7° MLAT) and Panagyurishte (PAG, 42.7° MLAT) station, indicating they were west of the meridian of substorm development.

The global picture of magnetic disturbances is presented in Fig. 3b, which shows instantaneous map of the distribution of magnetic vectors obtained by the SuperMAG network during the maximum of the bay at BJN (Fig. 3a) and in Fig. 3c, which shows the distributions of magnetic disturbances and field-aligned currents calculated using data obtained by the AMPERE satellites during the start of the first polar substorm. According to the SuperMAG maps, the westward electrojet developed in the evening sector in the narrow band of high latitudes of Scandinavia at 16:30 UT (i.e., during the night substorm maximum at TIK (Fig. 1b) and the intense electrojet at auroral latitudes of Siberia). These disturbances could be associated with the poleward leap of the night westward electrojet.

The magnetic disturbances during the onset of the polar substorm shown on the AMPERE maps (Fig. 3c) are characterized by the emergence of a vortex near Spitsbergen. This corresponds to the sharp local intensification of field-aligned currents in this region, which was likely a source of the polar substorm.

Figure 4 shows the development of magnetic disturbances during the second typical polar substorm observed at IMF $B_Z > 0$. As with the first substorm, the disturbance consisted of several peaks corresponding to the different intensifications (Fig. 4a). At ~20:35 UT, a negative bay appeared at BJN and Nordkapp (NOR, 68.2° MLAT) and moved poleward. The bay appeared at HOR, LYR, and NAL at ~20:50–20:55 UT. The second intensification began at BJN at ~21:15 UT, and it appeared at Hornsund (HOR, 74.5° MLAT), Longyearbyen (LYR, 75.6° MLAT), and NAL by ~21:20 UT (i.e., it was a typical polar substorm). At the stations of the subauroral zone (these data are not presented here), we observed positive magnetic bays (~20–30 nT) with almost twice the intensity as during the first substorm. However, the amplitudes of positive bays were much smaller at BOX–BEL in the middle latitudes (Fig. 4d), where they did not exceed ~8 nT in the *X*-component or ~5 nT in the *Y*-component. There were virtually no disturbances at lower latitudes (PAG) (Fig. 4d).

The global pattern of magnetic disturbances is presented in Figs. 4b, 4c. The SuperMAG map shows that the westward electrojet was observed in a very narrow band over Spitsbergen at 21:34 UT. Analysis of the AMPERE maps over the interval of 20:00 to 22:00 UT shows that the longitudinally spaced downward and upward field-aligned currents were observed in the confined region at lower latitudes (corresponding to BJN) at ~21:20 UT (the figure is not shown). The AMPERE maps show that the westward electrojet was over Spitsbergen during the interval of 21:26–21:36 UT (Fig. 4b), flowing between the downward (blue) and upward (red) field-aligned current.

RESULTS AND DISCUSSION

We considered two substorm disturbances that started at ~16:40 UT and ~21:30 UT and were observed over the Spitsbergen archipelago on December 17, 2012, with IMF $B_Z > 0$ and morphology typical of polar substorms.

However, the magnetic disturbances of the first polar substorm at ~16:40 UT resulted from a superpo-

sitioning of the evening disturbances in the region of the poleward leap associated with the night auroral substorm over Siberia, plus a new disturbance in the polar substorm caused by local intensification of the downward field-aligned currents in the vicinity of Spitsbergen and corresponding intensification of Pi2 and Pi1B geomagnetic pulsations. This led to the emergence of complex auroral forms. Note that similar events were considered in [12, 16]. It was shown in [16] that the auroras under these conditions took the form of a large-scale spiral structure.

The second substorm (at ~21:30 UT) was a classical polar substorm in which disturbances were recorded only at high latitudes and no unusual auroral forms were observed.

It was also unusual that during the polar substorm in the evening sector, an intense vortex in ground-based magnetic variations and a corresponding local surge of a strong upward current with a very weak downward current were observed in the region. This testifies to an intense precipitation of electrons, while the typical night substorm was characterized by the westward electrojet flowing between the downward (blue) and the upward (red) currents.

The substorms also differed in their midlatitude effects. During the evening substorm, positive bays were recorded at both subauroral and middle latitudes up to the PAG station (Bulgaria), and the amplitude of positive bays at middle latitudes was greater than at subauroral ones. A similar occurrence of positive bays in a wide range of latitudes was recorded in [16] during a polar substorm developing against the background of its preceding auroral activity.

During the second substorm (~21:30 UT), positive bays were observed mainly at subauroral and middle latitudes. We suggest that differences between the midlatitude effects of the two polar substorms were associated first with the activity that preceded them, and then with the low amplitude of the second polar substorm and the strong displacement of its center toward high latitudes.

CONCLUSIONS

A comparative analysis was performed for two polar substorms observed over the Spitsbergen archipelago at an IMF B_Z of >0. There was a typical polar substorm recorded around midnight on the contracted auroral oval under the preceding quiet conditions and an evening polar substorm caused by the intensification of field-aligned currents in the region of a poleward leap at the western edge of the night substorm electrojet at auroral latitudes. It was shown that under these complex conditions, the polar substorm differed from a typical substorm in several ways (the forms of the auroras, the field-aligned currents, and the midlatitude effects).

ACKNOWLEDGMENTS

We thank the anonymous reviewer for his/her helpful remarks.

We are grateful to the developers of the OMNI (http://omniweb.gsfc.nasa.gov), SuperMAG (http://supermag.jhuapl.edu/), IMAGE (http://space.fmi.fi/image/), and AMPERE (http://www.ampere.jhuapl.edu) databases for allowing us to use them in our work.

FUNDING

The work of I.V. Despirak and A.A. Lubchich in analyzing phenomena at high latitudes was performed as part of State Task for the Polar Geophysical Institute. Their work in analyzing phenomena at middle latitudes was supported by the Russian Foundation for Basic Research, project no. 20-55-18003-Bulg_a. The work of N.G. Kleimenova was supported by the Russian Foundation for Basic Research, project no. 20-55-18003Bulg_a. The work of L.M. Malysheva was performed as part of a State Task for the Schmidt Institute of Physics of the Earth. The work of L.I. Gromova was performed as part of a State Task for the Pushkov Institute of Terrestrial Magnetism, Ionosphere, and Radio Wave Propagation. The work of A.V. Roldugin and B.V. Kozelov was performed as part of a State Task for the Polar Geophysical Institute.

CONFLICT OF INTEREST

The authors declare that they have no conflicts of interest.

REFERENCES

1. Sergeev, V.A., Yakhnin, A.G., and Dmitrieva, N.P., *Geomagn. Aeron.*, 1979, vol. 19, no. 6, p. 1121.
2. Gussenhoven, M.S., *J. Geophys. Res.*, 1982, vol. 87, no. A4, p. 2401.
3. Despirak, I.V., Lubchich, A.A., Yahnin, A.G., et al., *Ann. Geophys.*, 2009, vol. 27, no. 5, p. 1951.
4. Despirak, I.V., Lubchich, A.A., Biernat, H.K., and Yahnin, A.G., *Geomagn. Aeron.*, 2008, vol. 48, no. 3, p. 284.
5. Feldstein, Y.L. and Starkov, G.V., *Planet. Space Sci.*, 1967, vol. 15, no. 2, p. 209.
6. Dmitrieva, N.P. and Sergeev, V.A., *Magnitos. Issled.*, 1984, no. 3, p. 58.
7. Nielsen, E., Bamber, J., Chen, Z.-S., et al., *Ann. Geophys.*, 1988, vol. 6, no. 5, p. 559.
8. Loomer, E.I. and Gupta, J.C., *J. Atmos. Terr. Phys.*, 1980, vol. 42, p. 645.
9. Yahnin, A.G., Despirak, I.V., Lubchich, A.A., and Kozelov, B.V., *Proc. 7th Int. Conf. on Substorms*, Levi, 2004, p. 31.

10. Akasofu, S.-I., Perreault, P.D., Yasuhara, F., and Meng, C.I., *J. Geophys. Res.*, 1973, vol. 78, no. 31, p. 7490.
11. Lui, A.T.Y., Akasofu, S.-I., Hones, E.W., Jr., et al., *J. Geophys. Res.*, 1976, vol. 81, no. 7, p. 1415.
12. Kleimenova, N.G., Antonova, E.E., Kozyreva, O.V., et al., *Geomagn. Aeron.*, 2012, vol. 52, no. 6, p. 746.
13. Despirak, I.V., Lyubchich, A.A., and Kleimenova, N.G., *Geomagn. Aeron.*, 2014, vol. 54, no. 5, p. 575.
14. Despirak, I.V., Lyubchich, A.A., and Kleimenova, N.G., *Geomagn. Aeron.*, 2019, vol. 59, no. 1, p. 1.
15. Despirak, I.V., Lubchich, A.A., and Kleimenova, N.G., *J. Atmos. Sol.-Terr. Phys.*, 2018, vol. 177, p. 54.
16. Safargaleev, V.V., Kozlovsky, A.E., and Mitrofanov, V.M., *Ann. Geophys.*, 2020, vol. 38, no. 4, p. 901.
17. Newell, P.T. and Gjerloev, J.W., *J. Geophys. Res.*, 2011, vol. 116, no. A12, A12221.
18. Viljanen, A. and Häkkinen, L., *ESA Publications SP-1198*, 1997, p. 111.
19. Anderson, B.J., Takanashi, K., and Toth, B.A., *Geophys. Rev. Lett.*, 2000, vol. 27, no. 24, p. 4045.
20. Clausen, L.B., Baker, J.B.H., Ruohoniemi, J.M., et al., *J. Geophys. Res.*, 2012, vol. 117, no. A6, A06233.
21. Kangas, J., Guglielmi, A., and Pokhotelov, O., *Space Sci. Rev.*, 1998, vol. 83, p. 435.
22. Kleimenova, N.G., *Geomagnitnye pul'satsii: Modeli kosmosa* (Geomagnetic Pulsations: Space Models), Moscow: MGU, 2007, vol. 1.
23. Pytte, T., McPherron, R.L., Kivelson, M.G., et al., *J. Geophys. Res.*, 1978, vol. 83, no. A11, p. 5256.

Translated by L. Mukhortova